Raman scattering from highly-stressed anvil diamond

Shan Liu(刘珊), Qiqi Tang(唐琦琪), Binbin Wu(吴彬彬), Feng Zhang(张峰), Jingyi Liu(刘静仪), Chunmei Fan(范春梅), and Li Lei(雷力)

Citation: Chin. Phys. B, 2021, 30 (**1**): 016301. DOI: 10.1088/1674-1056/abc7a7
Journal homepage: http://cpb.iphy.ac.cn; http://iopscience.iop.org/cpb

What follows is a list of articles you may be interested in

Raman scattering study of two-dimensional magnetic van der Waals compound VI_3

Yi-Meng Wang(王艺朦), Shang-Jie Tian(田尚杰), Cheng-He Li(李承贺), Feng Jin(金峰), Jian-Ting Ji(籍建葶), He-Chang Lei(雷和畅), Qing-Ming Zhang(张清明)

Chin. Phys. B, 2020, 29 (**5**): 056301. DOI: 10.1088/1674-1056/ab8215

Raman scattering study of magnetic layered MPS_3 crystals (M=Mn, Fe, Ni)

Yi-Meng Wang(王艺朦), Jian-Feng Zhang(张建丰), Cheng-He Li(李承贺), Xiao-Li Ma(马肖莉), Jian-Ting Ji(籍建葶), Feng Jin(金峰), He-Chang Lei(雷和畅), Kai Liu(刘凯), Wei-Lu Zhang(张玮璐), Qing-Ming Zhang(张清明)

Chin. Phys. B, 2019, 28 (**5**): 056301. DOI: 10.1088/1674-1056/28/5/056301

Bismuth-content-dependent polarized Raman spectrum of InPBi alloy

Guan-Nan Wei(魏冠男), Qing-Hai Tan(谭青海), Xing Dai(戴兴), Qi Feng(冯琦), Wen-Gang Luo(骆文刚), Yu Sheng(盛宇), Kai Wang(王凯), Wen-Wu Pan(潘文武), Li-Yao Zhang(张立瑶), Shu-Min Wang(王庶民), Kai-You Wang(王开友)

Chin. Phys. B, 2016, 25 (**6**): 066301. DOI: 10.1088/1674-1056/25/6/066301

Raman phonons in multiferroic $FeVO_4$ crystals

Zhang An-Min, Liu Kai, Ji Jian-Ting, He Chang-Zhen, Tian Yong, Jin Feng, Zhang Qing-Ming

Chin. Phys. B, 2015, 24 (**12**): 126301. DOI: 10.1088/1674-1056/24/12/126301

Effect of 6H-SiC (1120) substrate on epitaxial graphene revealed by Raman scattering

Lin Jing-Jing, Guo Li-Wei, Jia Yu-Ping, Chen Lian-Lian, Lu Wei, Huang Jiao, Chen Xiao-Long

Chin. Phys. B, 2013, 22 (**1**): 016301. DOI: 10.1088/1674-1056/22/1/016301

Raman scattering from highly-stressed anvil diamond*

Shan Liu(刘珊)[1], Qiqi Tang(唐琦琪)[1], Binbin Wu(吴彬彬)[1],
Feng Zhang(张峰)[1], Jingyi Liu(刘静仪)[1], Chunmei Fan(范春梅)[1], and Li Lei(雷力)[1,2,†]

[1] *Institute of Atomic and Molecular Physics, Sichuan University, Chengdu* 610065, *China*
[2] *Key Laboratory of High Energy Density Physics and Technology (Ministry of Education), Sichuan University, Chengdu* 610065, *China*

(Received 21 July 2020; revised manuscript received 21 October 2020; accepted manuscript online 5 November 2020)

The high-frequency edge of the first-order Raman mode of diamond reflects the stress state at the culet of anvil, and is often used for the pressure calibration in diamond anvil cell (DAC) experiments. Here we point out that the high-frequency edge of the diamond Raman phonon corresponds to the Brillouin zone (BZ) center Γ point as a function of pressure. The diamond Raman pressure gauge relies on the stability of crystal lattice of diamond under high stress. Upon the diamond anvil occurs failure under the uniaxial stress (197 GPa), the loss of intensity of the first-order Raman phonon and a stress-dependent broad Raman band centered at 600 cm^{-1} are observed, which is associated with a strain-induced local mode corresponding to the BZ edge phonon of the L_1 transverse acoustic phonon branch.

Keywords: diamond anvil cell, Raman scattering, pressure calibration, Brillouin zone

PACS: 63.20.–e, 63.50.–x, 78.30.–j **DOI:** 10.1088/1674-1056/abc7a7

1. Introduction

Diamond has a cubic crystal structure with space group *Fd*-3*m*, in which two carbon atoms are arranged in the primitive unit cell (Fig. 1(a)). For a perfect crystal, the phonon modes in the proximity of the center of the Brillouin zone (BZ) can only be observed owing to the $q \approx 0$ selection rule. Accordingly, the observed first-order Raman phonon at 1332 cm^{-1} corresponds to the Γ point of BZ center in the diamond crystal with F_{2g} symmetry (Fig. 1(b)). Under the uniaxial stress, the first-order Raman band of diamond exhibits asymmetry broadening and blue-shift, which is attributed to the strain effect that violates the translational invariance and breaks down the phonon wave vector selection rule.[1]

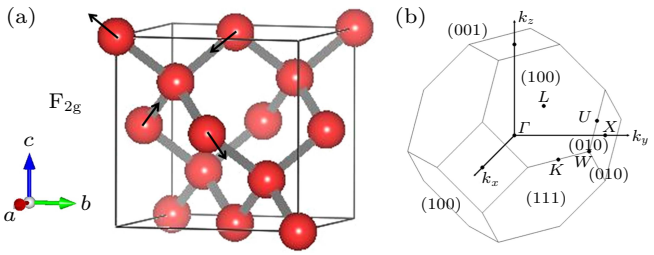

Fig. 1. (a) The crystal structure of cubic diamond, the black arrows indicate the Raman vibrational motions F_{2g}. (b) The Brillouin zone of cubic diamond.

Due to the ultra-high bulk modulus (450 GPa)[2] and ultra-high hardness ($H_v > 110$ GPa),[3] diamond single crystals with (100) crystal face are one of the best candidates for the anvil materials in the high-pressure experiments.[4] The high-frequency edge of the first-order Raman phonon in diamond reflects the stress state at the culet of anvil, and shows a monotonic pressure dependence of elastic strain. Therefore, the spectroscopic method based on the stress-induced diamond phonon is an effective pressure scale (> 100 GPa) in a diamond anvil cell (DAC) experiment.[5] However, the pressure-dependent shift of the high-frequency edge of diamond Raman is lack of detailed lattice dynamic analysis.

A new Raman band at ~ 600 cm^{-1} was observed in both the highly-stressed (above 150 GPa) diamond anvil[6] and the nano-sized diamond particles sample.[7] Both the strain effect and size effect can be attributed to the disordered Raman band at ~ 600 cm^{-1} in a phonon-confinement system. Typical examples of these systems include nano-sized crystals,[8,9] defect and impurity semiconductors,[10–12] highly-stressed[6] and structural-disordered materials.[13] By applying the relaxation of selection rule to all the phonon branches of BZ, many features like the redshift and the asymmetry broadening in the Raman spectrum of disordered carbon could be well explained.[13,14] Despite the progress achieved, the observed broad Raman band at ~ 600 cm^{-1} under highly-stressed condition is still lack of detailed lattice dynamic analysis.

In this work, the Raman scattering from a pair of anvil diamonds in DAC has been studied at pressure up to 197 GPa. Up to the maximum pressure, one of the opposed diamond anvils occurs failure but cannot lead directly to the burst of anvils, and the other one remains intact that can be used for pressure calibration by the first-order Raman phonon. In order to gain a better understanding of phonon behavior in diamond under extreme conditions, we perform careful lattice dynamic analysis on the pressure-dependent Raman phonon of anvil diamonds by comparing the phonon dispersion curves of the di-

*Project support by the National Natural Science Foundation of China (Grant No. 11774247).
†Corresponding author. E-mail: lei@scu.edu.cn

amond.

2. Experimental details

Raman scattering experiments were carried out on a custom-built confocal Raman spectrometry system in the backscattering geometry based on triple grating monochromator (Andor Shamrock SR-303i-B) with an attached EMCCD (Andor Newton DU970P-UVB); excitation was achieved by using a solid-state laser at 532 nm (RGB laser system) with laser power of 50 mW and collection by a 20×, 0.28 N.A. objective (Mitutoyo). The spectral resolution was within ± 1 cm^{-1}, and the spatial resolution was within ± 1 μm.

High-pressure Raman experiments were conducted at room temperature using a DAC with 50 μm culet (Fig. 2(a)) along the [100] diamond crystallographic direction (Fig. 2(a)). The diamond anvils were compressed across the rhenium gasket to the maximum pressure ($\sim$ 197 GPa) until plastic deformation and micro-cracks occurred on the top of the upper-anvil diamond. The culet surface of the upper-anvil diamond is no longer flat, exhibiting inhomogeneous light scattering, which is in sharp contrast with the lower-anvil diamond that was found still to be intact (Fig. 2(b)). The strain-induced cracks could not lead directly to the burst of anvils, but the cell pressure was found to suddenly drop to approximately 185 GPa. Upon slow decompression, numerous stepped cracks formed around the culets of the upper and lower anvils (Fig. 2(b)). When the pressure released to approximately 60 GPa, two intersecting longitudinal cracks were found in the upper-anvil diamond, with a consequent abrupt drop in the pressure value. This change indicates plastic deformation of the anvil tip, which has been documented for naturally deformed diamonds,[1] but not rarely identified *in situ* at high pressure.[6]

In the present study, the pressure was monitored through the high-frequency edge of the diamond phonon.[5] When the upper-anvil diamond occurs failure, the pressure calibration of DAC on decompression is only determined by the intact lower-anvil diamond. Here, the compressive stress of the upper-anvil diamond is considered to be equal to that of the lower-anvil diamond.

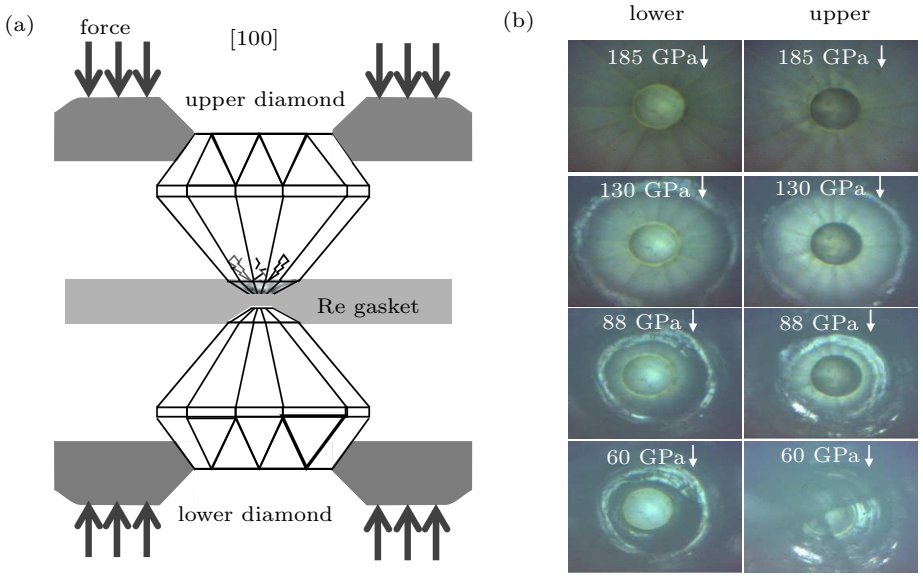

Fig. 2. (a) Schematic of the DAC geometry. (b) Selected microscope image of the lower- and upper-anvil diamonds on decompression. These images were acquired with the same light intensity.

3. Results and discussion

Spatially resolved micro-Raman spectra at the anvil tips provide direct information about the effect of normal stress on the diamonds. The first-order Raman phonon of diamond exhibits a sharp peak that corresponds to the triply degenerate optical phonons in the absence of stress. The uniaxial stress has been considered as the origin of the asymmetric broadening and blue-shift of the Raman phonon.[15–17] Under normal conditions, the first-order Raman phonon of anvil diamond shifts and splits under compression and decompression, meanwhile the second-order Raman phonons can also be clearly observed, as shown in Fig. 3(a). The cell pressure can be routinely calibrated by the high-frequency edge of the first-order Raman phonon.

In a typical ultrahigh-pressure DAC experiment, one of the two opposite diamonds occurs early failure at the maximum pressure, unavoidably disabling the pressure calibration process. In the present experiment, the exhausted upper-anvil diamond occurs failure at the pressure of 197 GPa. Subsequently, the pressure within the cell exhibits a sudden drop to $\sim$ 185 GPa (the pressure was only determined by the lower-anvil diamond). As a result, the first-order Raman peak becomes very week and the second-order Raman phonon cannot

be observed (Fig. 3(b)). At the same time, a strong broad peak centered at (ca.) ~ 600 cm^{-1} appears in the low-frequency region (Fig. 3(b)). Thus, the pressure calibration of DAC can only be speculated from the intact lower-anvil diamond (Fig. 3(a)). However, the pressure of the upper and lower anvils will not be exactly the same, so the pressure of the upper diamond is an approximate value.

The intensity of the broad-band is directly correlated to the stress on the anvil. A new broad Raman band at 600 cm^{-1} and the loss of intensity of the first-order Raman phonon in diamond were also observed by Mao *et al*. at sample pressures above 150 GPa.[6] Mao *et al*. considered that there was a close similarity between the new Raman feature and the one-phonon density of states of diamond (which has a broad peak centered at ~ 600 cm^{-1}). They also considered that the new band may be associated with the appearance of fluorescence.[6] But the similar broad Raman band at 600 cm^{-1} was observed in nano-sized diamond particles by Yoshikawa *et al*.[7] So the fluorescence mechanism was rule out. Both the strain effect and size effect can result in the low-frequency broad Raman band at ~ 600 cm^{-1}, as a matter of fact, it can be explained by the disordered-activated Raman scattering from a phonon-confinement system.

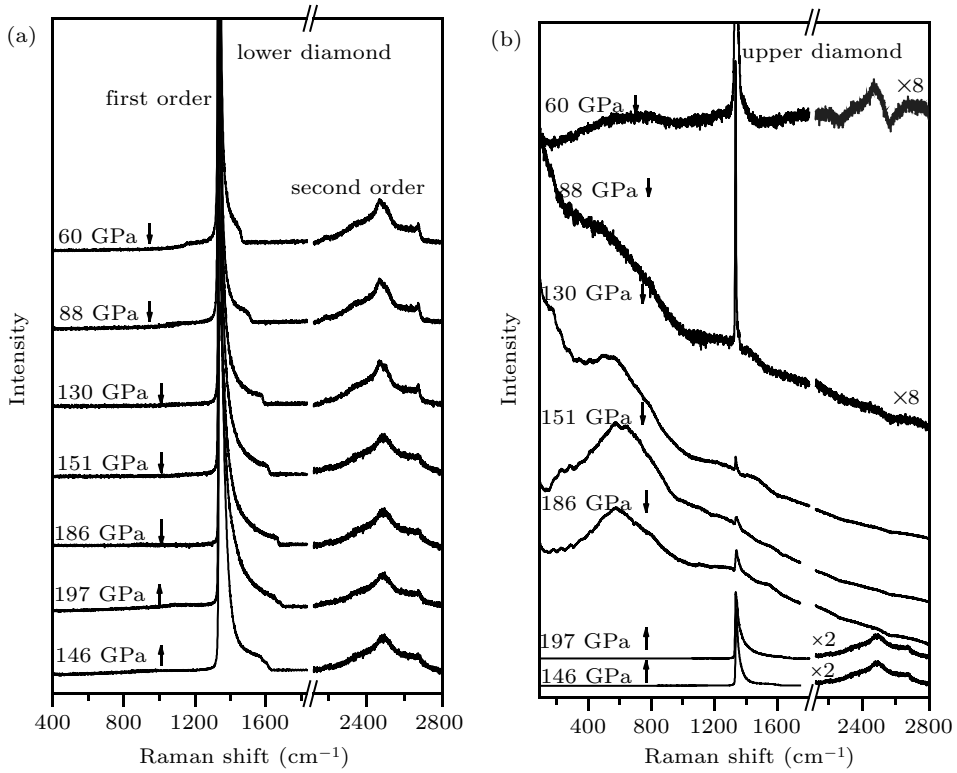

Fig. 3. (a) Pressure dependent Raman spectra of the lower-anvil diamond. (b) Pressure dependent Raman spectra of the upper-anvil diamond.

Figure 4(a) shows the pressure-dependent Raman spectra of the upper-anvil diamond collected during decompression. As the pressure decreases, the low-frequency Raman band redshifts and becomes weaker in intensity (Fig. 4(b)), while the first- and second-order diamond Raman modes have gradually recovered (Figs. 3(b) and 4(a)). At pressure below 100 GPa, the low-frequency mode becomes very weak; and at pressure below 60 GPa, the low-frequency mode almost disappears, but the first- and second-order Raman modes are clearly observed (Fig. 3(b)). It is shown that the low-frequency Raman broad band ca. 600 cm^{-1} exhibits pressure dependence. The emergence of such a local phonon is attributed to the strain-induced phonon confinements. The Raman selection rule is broken and the off-zone-center phonon modes are allowed. The disordered-activated Raman modes ca. 600 cm^{-1} were also observed in the doped diamond.[6,7] By comparing the vibrational frequency, the observed local phonon is consistent with the low-frequency phonon density of states (PDOS) of the perfect diamond (Fig. 4(a)). The PDOS is defined as the contribution from a given atom to the total phonon, describing the number of states per an interval of energy at each energy level available to be occupied. The disordered-activated phonon modes in disordered materials can be expressed by the PDOS of a corresponding perfect structure. Such a correlation could imply a breakdown in crystalline selection rules, resulting perhaps from growth of defects (stacking faults) at the anvil tips associated with macroscopic flow of the diamond, or from the formation of a new high-density amorphous form of carbon.[6]

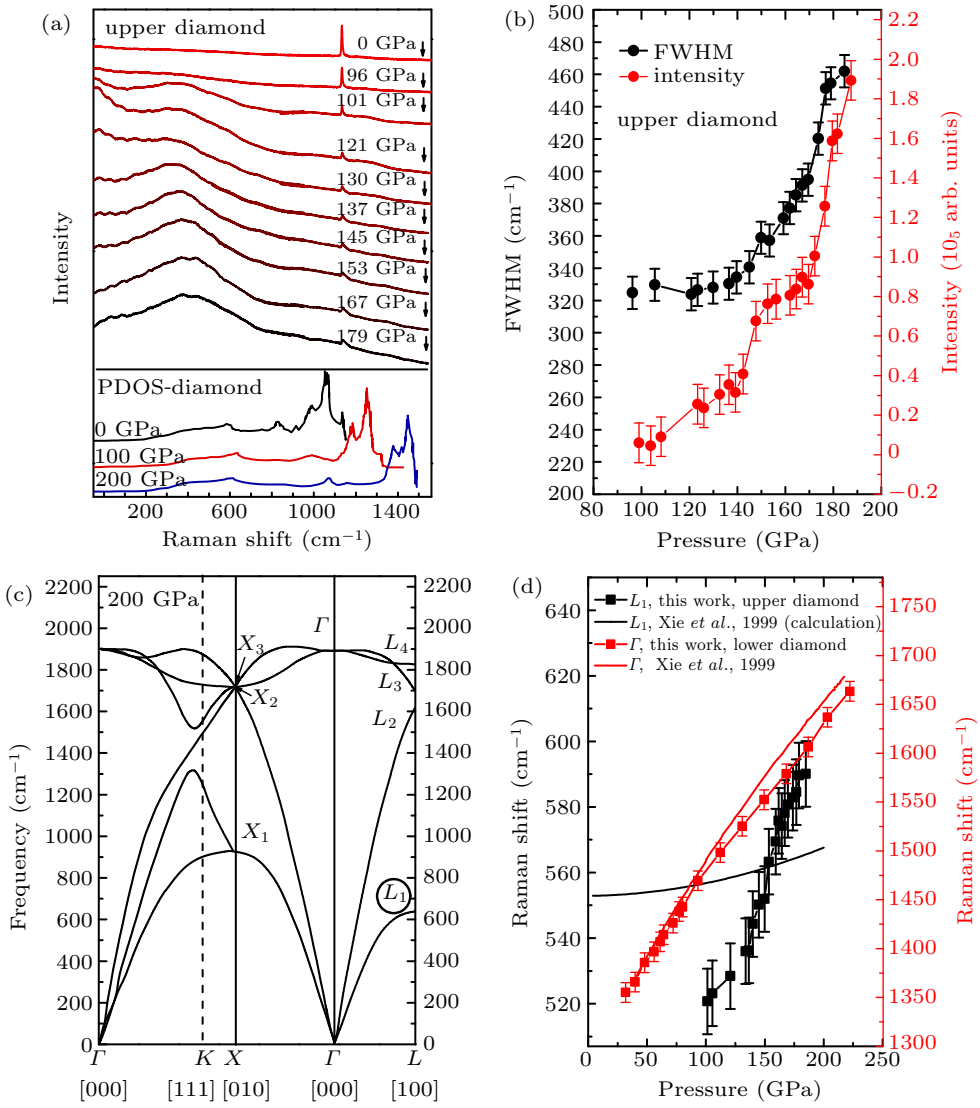

Fig. 4. (a) Pressure dependent Raman spectra of upper-anvil diamond on decompression. The black, red, and blue curves at the lower part represent the calculated PDOS[2] of diamond at 0 GPa, 100 GPa, and 200 GPa, respectively. (b) The full width at half maxima (FWHM) (black) and relative intensity (red) of local phonon as a function of pressure. (c) Phonon dispersion curves of diamond at $T = 300$ K, $P = 200$ GPa in different directions,[2] both the edge point L_1 and center point Γ are circled. (d) Comparison of experimental and calculated vibration frequencies for the edge point L_1 and center point Γ.

The high-frequency edge of the first-order Raman phonon of the diamond, which is often used to the pressure calibration, corresponds to the BZ center Γ point (Fig. 4(c)), and the high-frequency phonon edge of the first-order diamond exhibits very similar pressure dependence with the Γ point (Fig. 4(d)). The diamond Raman pressure gauge relies on the stability of crystal lattice of diamond under high stress. Plastic deformation induced by high stress leads to the inaccuracy and systematic deviation in the pressure calibration. By comparing with the calculated phonon dispersion curves of the diamond at 300 K, 200 GPa,[2] the observed low-frequency broad Raman mode corresponds to the strain-induced zone-edge phonon of the L_1 transverse acoustic phonon branch (Fig. 4(c)). Both the experimental and calculated values shift to lower energy with decreasing pressure (Fig. 4(d)). It is also noted that the L_1 zone edge branch corresponds to the [100] direction of the diamond (Fig. 1(b)), which corresponds to the experimental stress loading direction in the DAC (Fig. 2(a)).

4. Conclusion

We studied the pressure-dependent disordered Raman phonon behaviors of anvil diamond to 197 GPa, and observed a broad Raman mode centered at 600 cm^{-1} at the pressure above 100 GPa. The high-frequency edge of the first-order Raman phonon and the low-frequency broad Raman phonon were found to correspond to the zone center Γ point and the zone edge L_1 point, respectively. The diamond Raman pressure gauge relies on the stability of crystal lattice of diamond under high stress.

Acknowledgment

We thank Prof. Filippo Boi for helpful discussion.

References

[1] Pu M F, Zhang F, Liu S, Irifune T and Lei L 2019 *Chin. Phys. B* **28** 053102

[2] Xie J, Chen S P, Tse J S, de Gironcoli S and Baroni S 1999 *Phys. Rev. B* **60** 9444

[3] Brookes C A and Brookes E J 1991 *Diam. Relat. Mater.* **1** 13

[4] Jayaraman A 1983 *Rev. Mod. Phys.* **55** 65

[5] Akahama Y and Kawamura H 2004 *J. Appl. Phys.* **96** 3748

[6] Mao H K and Hemley R J 1991 *Nature* **351** 721

[7] Yoshikawa M, Mori Y, Maegawa. M, Katagiri G, Ishida H and lshitani A 1993 *Appl. Phys. Lett.* **62** 3114

[8] Korepanov V I and Hamaguchi H O 2017 *J. Raman Spectrosc.* **48** 842

[9] Zhao J, Pu M F, Liu S, Zhang F and Lei L 2019 *Mater. Res. Express* **6** 126502

[10] Prawer S and Nemanich R J 2004 *Phil. Trans. R. Soc. Lond. A* **362** 2537

[11] Mortet V, Živcová Z V, Taylor A, Frank O, Hubík P, Trémouilles D, Jomardf F, Barjonf J and Kavan L 2017 *Carbon* **115** 279

[12] Nemanich R J and Solin S A 1979 *Phys. Rev. B* **20** 392

[13] Lei L, Ohfuji H, Irifune T, Qin J, Zhang X and Shinmei T 2012 *J. Appl. Phys.* **112** 043501

[14] Ferrari A C and Robertson J 2000 *Phys. Rev. B* **61** 14095

[15] Cerdeira F, Buchenauer C J, Pollak F H and Cardona M 1972 *Phys. Rev. B* **5** 580

[16] Grimsditch M H, Anastassakis E and Cardona M 1978 *Phys. Rev. B* **18** 901

[17] Venugopalan S and Ramdas A K 1973 *Phys. Rev. B* **8** 717